Dislocation mutual interactions mediated by mobile impurities and the conditions for plastic instabilities

Fabio Leoni*
School of Mechanical Engineering, Tel-Aviv University, Tel-Aviv 69978, Israel

Stefano Zapperi
CNR-IENI, Via R. Cozzi 53, 20125 Milano, Italy and ISI Foundation, Via Alassio 11C, 10126 Torino, Italy

(Received 23 October 2013; published 7 February 2014)

Metallic alloys, such as Al and Cu or mild steel, display plastic instabilities in a well-defined range of temperatures and deformation rates, a phenomenon known as the Portevin–Le Chatelelier effect. The stick-slip behavior, or serration, typical of this effect is due to the discontinuous motion of dislocations as they interact with solute atoms. Here we study a simple model of interacting dislocations and show how the classical Einstein fluctuation-dissipation relation can be used to define the temperature over a range of model parameters and to construct a phase diagram of serration that can be compared to experimental results. Furthermore, by performing analytic calculations and numerically integrating the equations of motion, we clarify the crucial role played by dislocation mutual interactions in serration.

DOI: 10.1103/PhysRevE.89.022403 PACS number(s): 62.20.F−, 61.72.Bb, 66.30.J−, 61.72.Ff

I. INTRODUCTION

Dislocation dynamics is a complex intermittent phenomenon involving the collective motion of many dislocations interacting with each other as well as with obstacles eventually present in the material, such as solute atoms and quenched dislocations from other glide planes [1–3]. The long-range stress produced by dislocations may lead to jamming and avalanche-like phenomena even in the absence of obstacles [4]. The presence of obstacles changes the local properties of the host material, resulting in a pinning force on nearby dislocations [5,6]. Usually, this source of disorder for dislocations is taken to be quenched, so that its properties do not change within the relevant timescales of the system [7]. However, under specific conditions, the mobility of solute atoms in metallic alloys [8,9], or oxygen vacancies in superconductors [10], plays an important role in the dynamics of these systems.

Here we are interested in studying the dynamics of interacting dislocations mediated by mobile impurities. The interplay between dislocation mutual interactions and pinning by mobile impurities is believed to be at the origin of plastic instabilities observed in metallic alloys under suitable loading conditions and temperatures. One of the best-studied forms of instability propagation is the Portevin–Le Chatelier (PLC) effect [11–16]. When a specimen of a dilute alloy (such as an Al or Cu alloy or mild steel) is strained in uniaxial loading, the mechanical response is often discontinuous. In constant applied strain rate tests, the stress-versus-strain (or time, which is proportional to strain) curves exhibit a succession of stress drops and reloading sequences (serration).

From a dynamical point of view, the jerky or stick-slip behavior of stress is related to the discontinuous motion of dislocations, namely, the pinning (stick) and unpinning (slip) of dislocations. The classical explanation of the PLC effect is via the dynamic strain aging concept [17–24]. It is based on the interplay between the diffusivity of solute atoms and dislocations that can be arrested temporarily at obstacles during their waiting time. Thus, the longer the dislocations are arrested, the higher will be the stress required to unpin them. As a result, when the contribution from aging is large enough, the critical stress to move a dislocation increases with increasing waiting time or decreasing imposed strain rate. When these dislocations are unpinned, they move at a high speed until they are arrested again. At high strain rates (or low temperatures), the time available for solute atoms to diffuse towards the dislocations in order to age them decreases and hence the stress required to unpin them decreases. Thus, in the range of strain rates and temperatures where these two time scales are of the same order of magnitude, the PLC instability manifests. The competition between the slow rate of aging and the sudden unpinning of the dislocations translates, at the macroscopic level, into a negative strain rate sensitivity of the flow stress as a function of the strain rate [19]. This basic instability mechanism, used in most phenomenological models for the PLC effect [25], is based on the behavior of individual dislocation and thus does not explain how dislocation motion can synchronize to yield macroscopic strain bursts.

Current theoretical approaches to modeling the PLC effect are based on a mesoscopic descriptive level (where a coarse-grained dislocation density is considered) in which phenomenological parameters are needed to construct the relative dynamical equations [25]. Modeling plastic deformation phenomena taking into account inhomogeneity at the dislocation level offers fundamental advantages compared to continuum mechanics approaches. Discrete dislocation dynamical (DDD) approaches allow us, for example, to account for the intrinsic length scales, such as the grain size, the mesh length of a dislocation network, and the cross-slip height, which is necessary to understand the formation of spatial dislocation structures, such as persistent slip bands [26], and plastic instabilities, such as Lüders band and the PLC effect [25]. The problem of spatial and temporal coupling in heterogeneously deforming materials, and the associated length and time scales to be included in constitutive laws, is a central issue in

*gfabiol@gmail.com

current attempts to bridge a gap between dislocation-based constitutive models and continuum mechanics.

The general three-dimensional dynamical problem of dislocation lines interacting among each other is a complex problem due to the necessity of considering flexible lines, conserving their connectivity and line length, and taking care of line interactions [27–33]. In several instances, however, dislocations are arranged into regular structures that are amenable to analytic treatment and a more efficient simulation approach. Here we analyze the dynamics of the effective one-dimensional dislocation array called a pileup interacting with mobile impurities. A slip band can be envisaged as a queue of dislocations, a pileup, pushed through a series of obstacles (solute atoms or immobile dislocations from other glide planes). In our case the obstacles perform a diffusive motion, due to thermal effects, and interact with dislocations. This system can be viewed as a coupled one-dimensional channel of particles [34], in which particles in one channel (dislocations) are driven by an external force and experience a drag from the undriven particles (impurities) in the other channel. In the following we discuss the problem of a single dislocation in a cloud of mobile impurities, analyzed in Ref. [35], and then we propose a generalization of the equations in the case of many interacting dislocations in a landscape of mobile impurities.

II. SINGLE DISLOCATION INTERACTING WITH MOBILE IMPURITIES

Recently the dynamics of a particle interacting with diffusing impurities in one dimension has been investigated by Laurson and Alava [35]. Despite the simplicity of the model, which makes it analytically tractable, it exhibits a rich dynamics. Here we describe this model as an introduction to the following section, in which we generalize the relative equations to the case of many interacting dislocations.

In the full formulation of the model discussed in Ref. [35], a particle in a cloud composed of a fixed number of N_p impurities driven by an external force F is considered. The force is given by $F = k(Vt - x)$, where V is the driving velocity and k is a spring constant characterizing the response of the driving mechanism. The region of the parameter space is restricted to that in which the impurities have a vanishingly low probability of escaping from the vicinity of the particle within the time scale of the simulation. Thus, the particle is dragging an impurity cloud with a fixed number of impurity particles without escaping from it. The equations of motion are

$$\mu \frac{\partial x}{\partial t} = \sum_{i=1}^{N_p} f(x - x_{s,i}) + F,$$
$$\frac{\partial x_{s,i}}{\partial t} = -f(x - x_{s,i}) + \eta_i, \tag{1}$$

where x and x_s are the positions of the particle and the impurity particles, respectively. $f(z)$ is the interaction force between the particle and the impurity particle, μ defines the relative mobility of the impurity and the particle, and η_i are Gaussian white noise with standard deviation $\delta\eta$ and mean 0. The only condition imposed on the expression of the force $f(z)$ is $\partial_z f(z)|_{z=0} = -f_0$. Here we are interested, in particular, in the behavior of the external force F, which in experiments represents the shear stress acting on dislocations. For $z = x - x_s$ close to 0, the following expression for the stochastic process $\partial_t F$ is derived in Ref. [35]:

$$\partial_t^2 F = -k\partial_t^2 x = -\left[\frac{k}{\mu} + \frac{f_0}{\mu}(N_p + \mu)\right]\partial_t F + \frac{kf_0}{\mu}\sum_{i=1}^{N_p}\eta_i + \frac{kf_0}{\mu}[V(N_p + \mu) - F]. \tag{2}$$

Now, assuming that in the stationary state the last term on the right-hand side of Eq. (2) has 0 mean ($\langle V(N_p + \mu) - F\rangle = 0$) and that fluctuations are small compared to those of the white noise term ($\delta F \ll \sqrt{N_p}\delta\eta$), Eq. (2) reduces to the following Ornstein-Uhlenbeck process for $\partial_t F$:

$$\partial_t^2 F = -\left[\frac{k}{\mu} + \frac{f_0}{\mu}(N_p + \mu)\right]\partial_t F + \frac{kf_0}{\mu}\sum_{i=1}^{N_p}\eta_i. \tag{3}$$

The condition of small fluctuations $\delta F \ll \sqrt{N_p}\delta\eta$ is fulfilled for most of the relevant parameter value conditions; only for $kf_0 \gg 1$ is this not the case. From Eq. (3) it is possible to see that, after an initial transient, the system reaches the stationary state in which the external force F fluctuates around a constant average value and these fluctuations are uncorrelated in time [35]. Therefore, a system composed of a single dislocation in a cloud of mobile impurities does not display a serration-type behavior.

Equation (2) can be solved exactly, without imposing conditions on fluctuations. Indeed it is possible to rewrite it as a two-dimensional (2D) Ornstein-Uhlenbeck process. Introducing the new variable $F^* = F - V(N_p + \mu)$ and considering F^* and $\dot{F}^*$ as the components of a 2D vector, Eq. (2) can be written as a 2D Ornstein-Uhlenbeck process [36] for the vector variable $(F^*, \dot{F}^*)$,

$$\frac{d}{dt}\begin{pmatrix} F^* \\ \dot{F}^* \end{pmatrix} = -\begin{pmatrix} 0 & -1 \\ \omega_0^2 & \gamma \end{pmatrix}\begin{pmatrix} F^* \\ \dot{F}^* \end{pmatrix} + \begin{pmatrix} 0 \\ \Gamma(t) \end{pmatrix}, \tag{4}$$

where

$$\gamma = \frac{1}{\mu}[k + f_0(N_p + \mu)], \quad \omega_0^2 = \frac{kf_0}{\mu}, \quad \Gamma(t) = \frac{kf_0}{\mu}\sum_{i=1}^{N_p}\eta_i. \tag{5}$$

The solution for the average $\langle F^*\rangle$ is

$$\langle F^*\rangle = e^{-\boldsymbol{\gamma} t}\,|_{11}\; F^*(0) + e^{-\boldsymbol{\gamma} t}\,|_{12}\; \dot{F}^*(0), \tag{6}$$

where

$$F^*(0) = F(0) - V(N_p + \mu) = -V(N_p + \mu),$$
$$\dot{F}^*(0) = \dot{F}(0) = kV, \tag{7}$$

and matrix $\boldsymbol{\gamma}$ is

$$\boldsymbol{\gamma} = \begin{pmatrix} 0 & -1 \\ \omega_0^2 & \gamma \end{pmatrix}. \tag{8}$$

Diagonalizing the exponential matrix $e^{-\gamma t}$, we can write explicitly the expression of the average force $\langle F\rangle$ as

$$\begin{aligned}\langle F\rangle &= \langle F^*\rangle + V(N_p+\mu) = V(N_p+\mu)[1-e^{-\gamma t}|_{11}] + kVe^{-\gamma t}|_{12}\\ &= V(N_p+\mu)\left[1+\frac{\lambda_1 e^{-\lambda_2 t}-\lambda_2 e^{-\lambda_1 t}}{\lambda_1-\lambda_2}\right] + kV\left[\frac{e^{-\lambda_1 t}-e^{-\lambda_2 t}}{(\lambda_1-\lambda_2)t}\right],\end{aligned} \tag{9}$$

where $\lambda_{1,2}$ are the eigenvalues of $\boldsymbol{\gamma}$. The only case in which we can have fluctuations in the average force is obtained for $(\gamma^2-4\omega_0^2)<0$, which leads to the expression

$$\langle F\rangle = V(N_p+\mu)\left\{1+e^{-\frac{\gamma}{2}t}\left[\frac{\gamma}{2}\frac{\sin\left(\sqrt{4\omega_0^2-\gamma^2}t/2\right)}{\sqrt{4\omega_0^2-\gamma^2}/2}-\cos\left(\sqrt{4\omega_0^2-\gamma^2}t/2\right)\right]\right\} - kVe^{-\frac{\gamma}{2}t}\frac{\sin\left(\sqrt{4\omega_0^2-\gamma^2}t/2\right)}{\sqrt{4\omega_0^2-\gamma^2}t/2}. \tag{10}$$

In this case oscillations (serration) emerge, but they decay exponentially rapidly. On the other hand, performing the stationary limit, one finds

$$\lim_{t\to\infty}\langle F\rangle = V(N_p+\mu). \tag{11}$$

Therefore, for any parameter value conditions, serration-type behavior is not observed in the model of a single dislocation in a cloud of mobile impurities.

III. DISLOCATION PILEUP INTERACTING WITH MOBILE IMPURITIES

As the PLC effect is widely believed to be due to the dynamic interaction of dislocations with diffusing solute atoms, a natural formulation of the problem, in the framework of the DDD approach, is to consider Eq. (1) for N dislocations in a landscape of N_p mobile impurities. To describe the dynamics of dislocations we use, as in [35], an overdamped equation, so that the velocity of a dislocation depends linearly on the resolved shear stress exerted on it [37]. Therefore, the equations of motion, Eq. (1), are generalized as

$$\begin{aligned}\mu\frac{dx_i}{dt} &= G\sum_{\substack{j=1\\(j\neq i)}}^{N}\frac{b_ib_j}{x_i-x_j} + b_i\sigma_i^l + \sum_{j=1}^{N_p} f_P(x_i-x_{s,j}),\\ \chi\frac{dx_{s,j}}{dt} &= -\sum_{i=1}^{N} f_P(x_i-x_{s,j}) + \eta_j,\end{aligned} \tag{12}$$

where G is the shear modulus, b_i is the Burgers vector of the dislocation i, and μ and χ are the damping constant of dislocations and impurities respectively. The external force F is now explicitly indicated as the local shear stress σ_i^l acting on each dislocation i, whose expression is

$$\sigma_i^l = k\left[Vt-\int_0^t b_i\frac{dx_i(t')}{dt'}dt'\right] = k[Vt-b_i(x_i(t)-x_i(0))], \tag{13}$$

while for the pinning force $f_P(z)$, with $z=x_i-x_{s,j}$, and the noise term η_j we have the expressions

$$\begin{aligned} f_P(z) &= -f_0\frac{z}{\xi_P}e^{-(z/\xi_P)^2}, \quad \langle\eta_j(t)\rangle = 0,\\ \langle\eta_j(t)\eta_j(t')\rangle &= D\delta(t-t')\delta_{ij}.\end{aligned} \tag{14}$$

The detailed shape of the interaction force $f_P(z)$ is inessential for most purposes, provided it is of a short-range nature. As done in other similar work, we have chosen for $f_P(z)$ a function that satisfies this requirement and that is regular (derivable). To emulate the behavior of a material in the bulk, we consider that N point dislocations and N_p impurities move along a line of size L when periodic boundary conditions are chosen. In order to correctly take into account the effect of periodic boundary conditions, the interactions between dislocations are summed over their images [38].

We are interested in the total average stress exerted on dislocations, $\sigma = 1/N\sum_{i=1}^{N}\sigma_i^l$ (i.e., the external stress that must be applied to the material to obtain a constant strain rate). To study the behavior of the stress σ in relation to the PLC effect, which is regulated principally by the temperature and strain rate as discussed in Sec. I, we have imposed the relations $b_i=b=1$, $G=\mu=\xi_P=1$, $f_0=0.01$, and $k=0.1$, which fix the time, space, and force scales. The free parameters of the model are now V, χ, and D. In real materials impurities have already exerted aging effects over dislocations before the experiments (i.e., before an external stress is imposed on the material). To take this effect into account the system is left to evolve without external stress ($k=0$) for a waiting time t_w. The initial configuration of the system (at time $t=0$) consists of a random distribution of dislocations and pinning centers. We choose $t_w = 10^6\times dt = 10^4$, where the integration step is $dt=10^{-2}$. This value of t_w is sufficient for the system to stabilize its elastic energy during the initial part of the dynamics (for $t<t_w$ and $k=0$) [1].

IV. THE CONDITIONS FOR SERRATION

Before integrating numerically Eqs. (12), (13), and (14), we can obtain a set of necessary conditions for serration. First, we can observe that if dislocations do not interact with any pinning center [$f_P(z)=0$], the first Eq. (12) does not possess normal modes of oscillation. This can be found by employing a linear perturbative approach, as done in Ref. [39] to study the discrete cosmological N-body problem, or observing that the first Eq. (12) describes the so-called Coulomb gas for the variables $x_i-(V/b)t$ at 0 temperature [40].

If we now consider that dislocations interact with pinning centers [$f_P(z)\neq 0$], but with the last ones quenched (that means $dx_{s,j}/dt = 0$), from Eqs. (12)–(14) we obtain

$$\mu \frac{dx}{dt} = b\sigma + \frac{1}{N}\sum_{i=1}^{N}\sum_{j=1}^{N_p} f_P(x_i - x_{s,j}),$$
$$x_{s,j} = c_j,$$
$$\Longrightarrow \partial_t \sigma = kV - \frac{kb^2}{\mu}\sigma + \Gamma(t,\sigma_i^l,c_j) \quad (15)$$

where c_j are constants and the function Γ can be obtained using the relation between x_i and σ_i^l in Eq. (13). Performing the ensemble average and the time integral in Eq. (15), we obtain that $\langle\sigma\rangle = \mu V/b^2$ (so we do not have serration) if $\langle\Gamma\rangle = 0$, that is, if the constants c_j do not correlate the variables σ_i^l between them [i.e., if the c_j do not depend in a specific way on the position of the variables $x_i(0)$]. To find this result we employed the relation $\sum_{i=1(i\neq j)}^{N}\sum_{j=1}^{N} 1/(x_i - x_j) = 0$, introduced the variable $x = 1/N\sum_{i=1}^{N} x_i$, and considered the ensemble average with respect to the $\{c_j\}$ configurations.

Another necessary condition for serration can be found by observing that in the range of parameters for which the impurities have a vanishingly low probability of escaping from dislocations (the same case studied in Ref. [35] for the single-dislocation problem), we can approximate the expression of the interacting force $f(z)$ for small z as $f_P(z) \simeq f_P(0) + z\partial_z f_P(z)|_{z=0} = -f_0 z$. Employing this approximation, from Eqs. (12)–(14), we find for σ the following 2D Ornstein-Uhlenbeck equation:

$$\partial_t^2\sigma = -\frac{1}{\mu}\left[kb^2 + f_0N_p + \frac{f_0\mu N}{\chi}\right]\partial_t\sigma - \frac{f_0kb^2N}{\mu\chi}\sigma + \frac{f_0k}{\mu}\left[V\left(N_p + \frac{\mu N}{\chi}\right) + \frac{kb^3N}{\chi}x(0)\right] - \frac{f_0kb}{\mu\chi}\sum_{i=1}^{N_p}\eta_i, \quad (16)$$

which does not display serration as shown above. To obtain Eq. (16), the relations $\sum_{i=1(i\neq j)}^{N}\sum_{j=1}^{N} 1/(x_i - x_j) = 0$ and $\sum_{i=1(i\neq j)}^{N}\sum_{j=1}^{N} \partial_t(x_i - x_j)/(x_i - x_j)^2 = 0$ were employed.

Finally, from Eqs. (12)–(14) we have found four conditions necessary for serration. (i) First, the system must be composed of more than one dislocation [as found in Ref. [35] in the low-noise limit and as results in the general case from Eq. (11)]. In other words, serration in the stress response of the system, when present, comes from a collective effect of many interacting dislocations. To verify this, we studied the role of the interaction force between dislocations, analyzing the average stress $\langle\sigma\rangle$ as a function of time (or strain) for different values of the interaction force itself (obtained by changing the value of the shear modulus G), for parameter values at which serration is observed [$\mu/\chi = 0.5$, $1/T = 10^4$ (see the definition of T below), and $V = 0.003$]. In Fig. 1 we displayed the average stress $\langle\sigma\rangle$ (performed on 50 samples) as a function of time obtained by integrating numerically Eqs. (12) and (13). From it we can see that serration disappears when the strength of the interaction force between dislocations decreases. In particular, for vanishing interaction force ($G = 0$), the stationary average stress is given by the expression $\langle\sigma\rangle_s = V[(N_p/N)\chi + \mu] \simeq 0.051$, as

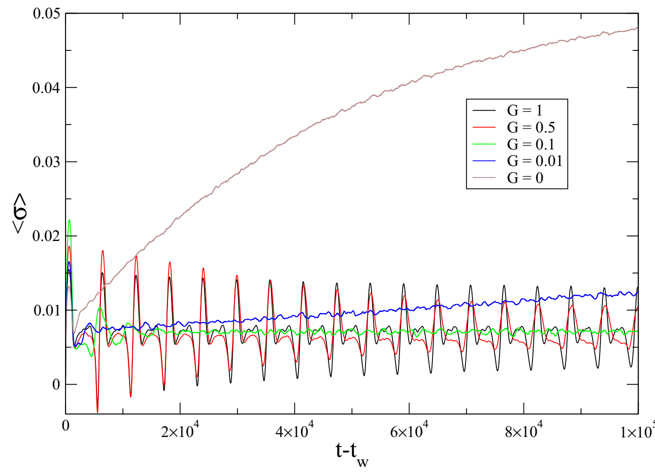

FIG. 1. (Color online) Average stress $\langle\sigma\rangle$ (performed on 50 samples) as a function of time obtained by integrating numerically Eqs. (12) and (13). The parameters of the system ($\mu/\chi = 0.5$, $1/T = 10^4$, and $V = 0.003$) are chosen in the range in which serration is observed in order to investigate the role of the interaction force between dislocations changing the value of the shear modulus G. From it we can see that serration disappears when the strength of the interaction force between dislocations decreases.

discussed in the following analysis of Fig. 2. (ii) Dislocations must interact with pinning centers. (iii) Pinning centers must not all be quenched [see Eq. (15)]. (iv) Finally, dislocations must not all be pinned by impurities [see Eq. (16)]. These conditions are all in agreement with the dynamic strain aging concept.

In order to verify the four conditions necessary for serration, and to investigate the behavior of the system in the entire free parameter space (V,χ,D), we integrated numerically Eqs. (12) and (13) using the Euler method with the fixed step $dt = 0.01$. We considered $N = 32$ dislocations with an average spacing $d = 16$ and average pinning center spacing $d_p = L/N_p = 2$. Because $L = dN$, $N_p = dN/d_p = 8N$. Instead of using the set of parameters (V,χ,D), we employed the set $(V,\mu/\chi,1/T)$, where T is the temperature of the system defined in the following. Although we choose, without loss of generality, $\mu = 1$, we prefer to keep explicitly the ratio μ/χ. On the other hand, the explicit introduction of the temperature variable permits us to compare the phase diagram of the PLC effect (in Fig. 3) with results in the literature [41]. The definition of temperature is not something obvious in DDD models. Here we introduce the temperature T of the system as obtained from the Einstein fluctuation-dissipation relation: $T = 2D/\chi$. One difficulty in deriving a general theory of plasticity is due to the presence of thermal as well as athermal dislocation activated processes [25]. For this reason a clear definition of temperature in DDD models is still lacking. The simple one we use here can be considered a good definition for high temperatures, disregarding the possibility of cross-slip, and low stresses, in which case diffusional deformation mechanisms become predominant [1]. In any case, we analyze the system over the entire range of parameter values and we discuss, in the regimes in which this definition of T is not a good approximation, how it is related to the behavior of the system.

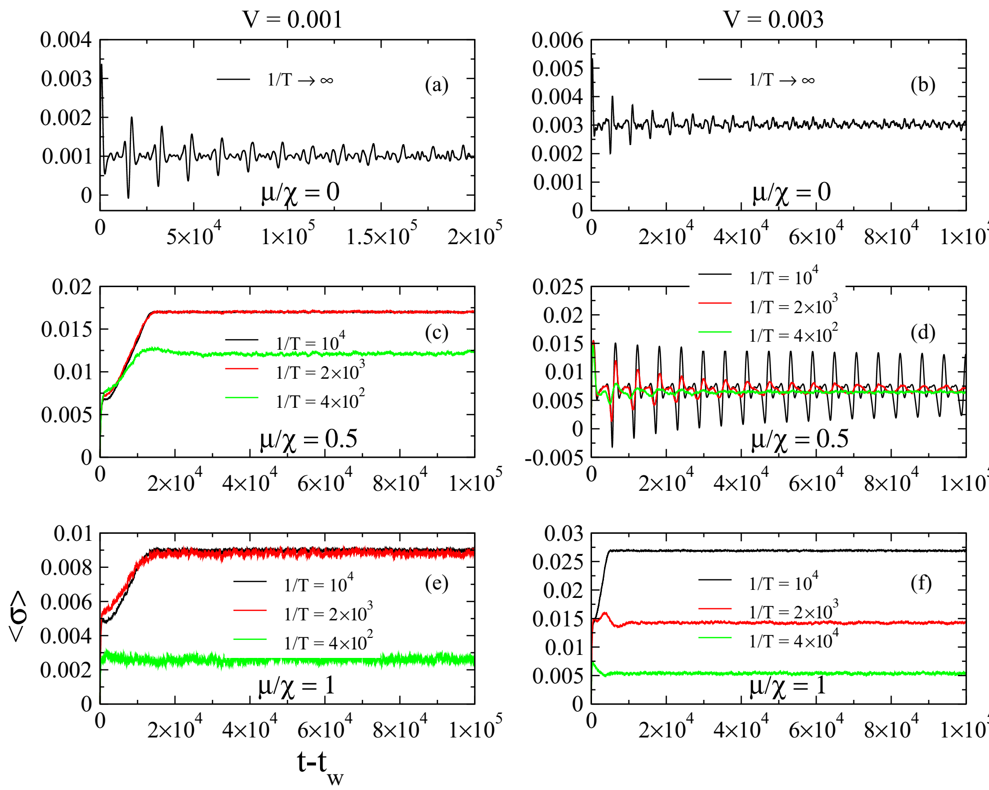

FIG. 2. (Color online) Average stress $\langle\sigma\rangle$, obtained by integrating numerically Eqs. (12) and (13), as a function of time $t - t_w$, for $t_w = 10^6 \times dt = 10^4$, driving velocity $V = 0.001$ and 0.003, mobility ratio $\mu/\chi = 0$, 0.5, and 1, and inverse temperature $1/T \to \infty$ and $1/T = 10^4$, 2×10^3, and 4×10^2.

In Fig. 2 the average stress $\langle\sigma\rangle$, obtained by integrating numerically Eqs. (12) and (13), as a function of time $t - t_w$ is plotted for driving velocity $V = 0.001$ and 0.003, mobility ratio $\mu/\chi = 0, 0.5$, and 1, and inverse temperature $1/T \to \infty$ and $1/T = 10^4$, 2×10^3, and 4×10^2. The average $\langle\cdot\rangle$ is performed on 50 samples. In the analysis in Fig. 2 we distinguish two cases: the first for $\mu/\chi = 0$ and the second for $\mu/\chi > 0$. The case $\mu/\chi = 0$ corresponds to quenched pinning centers [$dx_{s,j}/dt = 0$; see Eq. (15)]. From Figs. 2(a) and 2(b) we see that for $\mu/\chi = 0$, the average stress, after oscillations decreasing in time, reach the stationary value $\langle\sigma\rangle_s = \lim_{t\to\infty}\langle\sigma\rangle = V\mu$.

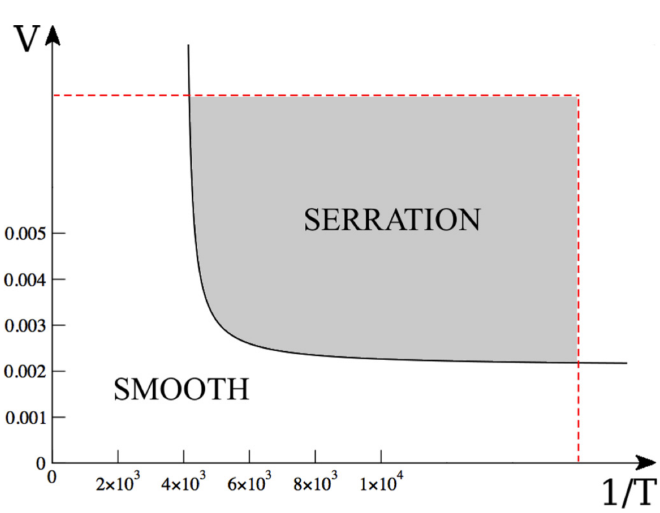

FIG. 3. (Color online) Semiquantitative phase diagram for the PLC effect in the parameter space $(1/T,V)$ for $\mu/\chi = 0.5$. In the range of parameters inside the shaded (gray) region, the PLC effect takes place (i.e., the average stress $\langle\sigma\rangle$ displays serration). Dashed (red) lines indicate where the model described by Eqs. (12) and (13) start to fail in predicting the PLC effect.

In the case of $\mu/\chi > 0$ we expect that at low temperatures and low driving velocities, or at low temperatures and high driving velocities, but high values of mobility ratio, dislocations are pinned by impurities. This is confirmed in Figs. 2(c)–2(f), from which we can see that the stationary value of the average stress is given by the relation $\langle\sigma\rangle_s = V[(N_p/N)\chi + \mu]$, as can be obtained from Eq. (16). To understand the role of dislocation interaction when they are pinned during the whole dynamics, we can consider Eq. (11) obtained for the dynamics of a single dislocation generalized to the case in which the damping constant of each impurity is χ. Therefore the expression of the stationary external force becomes $\lim_{t\to\infty}\langle F\rangle = V(N_p\chi + \mu)$, in which N_p is the number of impurities around the only present dislocation. In the case of N dislocations pinned by N_p impurities over the whole dynamics, we have that on average each dislocation i is pinned by N_p/N impurities (considering that the initial spatial distribution of dislocations and pinning centers is a random flat one). If we now suppose that under these conditions (obstacles that cannot unpin from dislocations), dislocations do not fluctuate too much around their equilibrium positions (which is a configuration of equidistant dislocations), we can conclude that the average stationary stress can be obtained from the formula for the case of a single dislocation pinned by N_P/N obstacles. This means that $\langle\sigma\rangle_s = \langle F(N_p \to N_p/N)\rangle_s$, which can be verified by employing the previous generalized version of Eq. (11). When T or V increases, the number of impurities that pin dislocations decreases, so $\langle\sigma\rangle_s$ decreases.

In Fig. 2 we can see that stationary fluctuations in the stress (serration) emerge for the parameter values $V = 0.003$, $\mu/\chi = 0.5$, and $1/T = 10^4$. In Fig. 2 results for driving velocities higher than $V = 0.003$ and temperatures T lower than 10^{-4} are not reported because in these regimes we reach the limit of our model, which continues to give serration in the stationary average stress, while in real systems we would not have serration [25,41]. Negative values of stress fluctuations at the earliest times correspond to sudden increases in the dislocation average position [see Eq. (13)], which happen when dislocations escape from many pinning centers. Indeed, when it happens, we can observe this effect at the earliest times of the dynamics (for $t > t_w$), because the absence of external stress for $0 < t < t_w$ permits dislocations to accumulate pinning centers. To verify that finite-size effects do not affect our results, we performed simulations for systems of $N = 16$, 32, 48, and 64 dislocations. We found that oscillations in the serration regime become bigger with increasing N, especially in the initial part of the dynamics, while after the order of 10 oscillations the serration stabilizes already for $N = 32$. The reason that oscillations become bigger with increasing N in the initial part of the dynamics is probably related to the fact that increasing the value of N_p, even though the average pinning center spacing does not change, increases the probability of a dislocation collecting a large number of pinning centers during the waiting time (from $t = 0$ to $t = t_w$). This probability should saturate with increasing system size (that is, increasing N). We suggest a more systematic finite-size analysis for a possible future work aimed at improving this model.

In order to summarize the results obtained from the present model and to compare them with experimental [41] and other theoretical [25] approaches, we depict in Fig. 3, relying on data displayed in Fig. 2 and other data not displayed there, a phase diagram for the PLC effect in the parameter space $(1/T,V)$ for $\mu/\chi = 0.5$. In the range of parameters within the shaded (gray) region, the PLC effect takes place. The dashed (red) lines indicate where the model described by Eqs. (12) and (13) starts to fail in predicting the PLC effect. In particular, for high driving velocities new dislocation mechanisms, such as dislocation multiplication, climbing, and other complex behaviors, must be taken into account. Considering these mechanisms, serration must disappear for high driving velocities irrespective of the other parameter values. However, in the case of low temperatures, nonthermal dislocation processes become relevant in relation to thermal ones, and the Einstein fluctuation-dissipation relation does not hold anymore. Also in this case, considering the presence of nonthermal dislocation processes, serration must disappear at low temperatures irrespective of the other parameter values.

The phase diagram of the PLC effect in the parameter space $(1/T,V)$, as depicted in Fig. 3, can also be analyzed in the framework of the self-organized avalanche oscillator approach recently introduced in Ref. [42]. Indeed, in that work it is shown that in a physical system under slowly increasing stress, in which fast and slow degrees of freedom are normally averaged out, if the slow degrees of freedom rearrange the pinning landscape at rates comparable to the external field driving rates, these slow processes can affect the behavior of the system, which can depend on these slow process rates. In our case, the external field driving rate is V, while the rearranging rate of the pinning landscape is related to the temperature T.

V. THE RELEVANT TIME SCALES IN SERRATION

The behavior of the system described by Eqs. (12)–(14) can be analyzed in terms of time scales. The fundamental time scales are: (i) the capturing time t_c, which accounts for the average time needed for a dislocation to capture a pinning center; and (ii) the aging time t_a, which accounts for the average time needed for a dislocation to escape from a pinning center. In order to compute these times we consider that a pinning center pins a dislocation if the distance between them is smaller then $\xi_c = 3\xi_P = 3$ (otherwise the attraction force between them is considered negligible). In Table I we report the time ratio t_a/t_c for the same values of driving velocity V, mobility ratio μ/χ, and inverse temperature $1/T$ for which the average stress $\langle\sigma\rangle$ was computed and is displayed in Fig. 2. First, we can observe that for $V \to \infty$ or $\mu/\chi \to 0$ or $1/T \to 0$, the time ratio becomes $t_a/t_c = (2 \cdot \xi_c)/(d - 2 \cdot \xi_c) = 0.6$, where d is the dislocation average interdistance. Indeed, under these conditions we can consider the pinning centers to be fixed wih respect to dislocations (or vice versa) during the dynamics and the ratio t_a/t_c becomes nothing more than the ratio between the average (in time) length per dislocation and pinning center over which dislocations are considered pinned [that is, $\alpha(t_{\rm av}) \cdot 2 \cdot \xi_c$] to that over which they are not [that is $\alpha(t_{\rm av}) \cdot (d - 2 \cdot \xi_c)$], where $\alpha(t_{\rm av})$ is the same parameter for the two lengths and depends only on the time $t_{\rm av}$ over which the average is performed. Looking at the values listed in Table I, we can observe that in general the time ratio t_a/t_c decreases significantly as V increases, or as μ/χ or $1/T$ decreases, but only for $\mu/\chi = 0.5$ and $V = 0.003$ do we have that t_a/t_c remains small (larger than, but near, the value 0.6) with changing $1/T$. In particular, for $\mu/\chi = 0.5$, $V = 0.003$, and $1/T = 10^4$ and 2×10^3, the two times t_a and t_c (whose ratio is displayed in Table I) are of the same order of magnitude, but the pinning centers, for these parameter values, are not fixed with respect to dislocations (or vice versa).

Finally, we can conclude that for the parameter values of V, μ/χ, and $1/T$ for which serration is observed, we have that the

TABLE I. Time scale ratio: t_a/t_c. The computational error is 1 over the last digit.

	$V = 0.001$		$V = 0.003$	
$\mu/\chi = 0$	0.60	for all $1/T$	0.60	for all $1/T$
$\mu/\chi = 0.5$	65.07	$1/T = 10^4$	**0.75**	$1/T = 10^4$
	66.48	$1/T = 2 \times 10^3$	**0.75**	$1/T = 2 \times 10^3$
	4.09	$1/T = 4 \times 10^2$	0.64	$1/T = 4 \times 10^2$
$\mu/\chi = 1$	78.73	$1/T = 10^4$	146.97	$1/T = 10^4$
	37.93	$1/T = 2 \times 10^3$	2.03	$1/T = 2 \times 10^3$
	1.13	$1/T = 4 \times 10^2$	0.79	$1/T = 4 \times 10^2$

two relevant times t_a and t_c are of the same order of magnitude (remembering that the value 0.6 corresponds to a special case in our model). This is in agreement with phenomenological models [25] and represents a link between microscopic DDD model parameters [appearing in Eqs. (12)–(14)] from which the quantities t_a and t_c can be computed and macroscopic quantities like V, μ/χ, and T.

VI. SPATIOTEMPORAL DISTRIBUTION OF DISLOCATIONS AND IMPURITIES

Analyzing spatiotemporal distributions of pinning centers and dislocations can help us to better understand and unify previous considerations and results. First, we computed the average pinning center distribution $\rho_{\text{p.c.}}$, averaging each distribution of pinning centers around every dislocation and averaging over 50 different realizations of the dynamics. In the lower panels in Fig. 4 we display the average pinning center distributions around dislocations for different times that correspond to different values of the average stress (these values are displayed in the stress vs time graphic in the top panel). The most interesting case, reported in Fig. 4 and corresponding to Fig. 2(d), is that for which a changing temperature causes the appearance or disappearance of serration (that is, for $\mu/\chi = 0.5$, $V = 0.003$). The distributions $\rho_{p.c.}$ are un-normalized so that the average number of pinning centers that pins dislocations is obtained by the integral $\int_{-\xi_c}^{\xi_c} \rho_{\text{p.c.}}(x_{\text{p.c.}}) dx_{\text{p.c.}} = \langle N_p \rangle$. To understand what happens when serration in the stress appears, we report in Fig. 4 the distributions in correspondence of stress drop, bump, and redrop. For temperatures for which the stress does not develop serration (for $1/T = 4 \times 10^2$ and 2×10^3), the distribution shape of pinning centers around dislocations does not change in time and displays a peak more or less wide or narrow depending on the values of V, μ/χ, and $1/T$. For temperatures at which serration develops (for $1/T = 10^4$), the distributions change in such a way that when pinning centers reach dislocations from the right side (indeed $V = 0.003 > 0$) [Fig. 4(b)] and start to pin them, stress drops because dislocations are accelerated [see Eq. (13)], then after a while the dislocation velocities go down because they are pinned (when the corresponding distribution has developed a high and narrow peak) [Figs. 4(c) and 4(d)]. Finally, when dislocations are able to depin and then their velocities start to increase again, the stress redrops [Figs. 4(e) and 4(f)].

Above, analyzing the stationary value of the stress (Fig. 2), we have argued that at low temperatures [in Figs. 2(c)–2(f)] dislocations are completely pinned and have verified that by means of the formula $\langle\sigma\rangle_s = V[(N_p/N)\chi + \mu]$, previously obtained from the equations of motion imposing the condition of complete pinning. Integrating the distributions of pinning centers, $\rho_{\text{p.c.}}$, for low temperatures, we can obtain the average

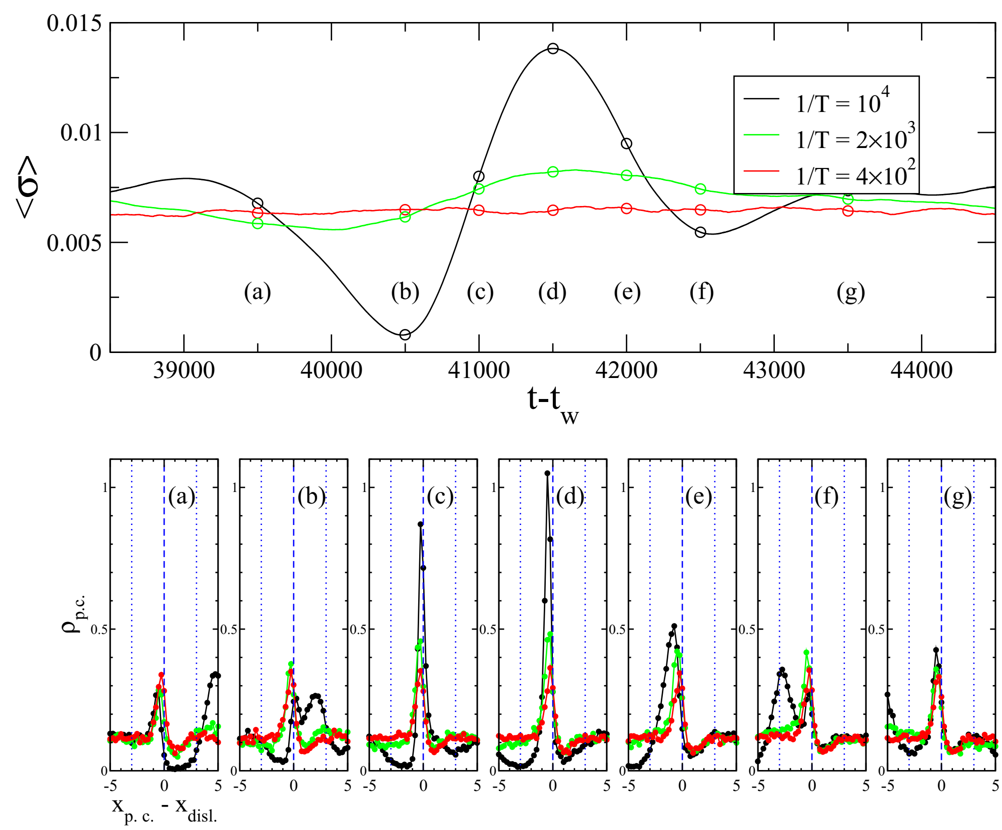

FIG. 4. (Color online) Spatiotemporal distribution of pinning centers around dislocations. The distributions are obtained by averaging for a specific time the different distributions around every dislocation and averaging over 50 different realizations of the dynamics. $x_{\text{p.c.}}$, pinning center position; $x_{\text{disl.}}$, dislocation position. The dashed vertical (blue) line indicates the dislocation position and the two dotted vertical (blue) lines indicate the cutoff ξ_c of the dislocation-pinning center interaction. In the upper panel, the average stress for a specific time region is indicated. The corresponding complete curve is shown in Fig. 2.

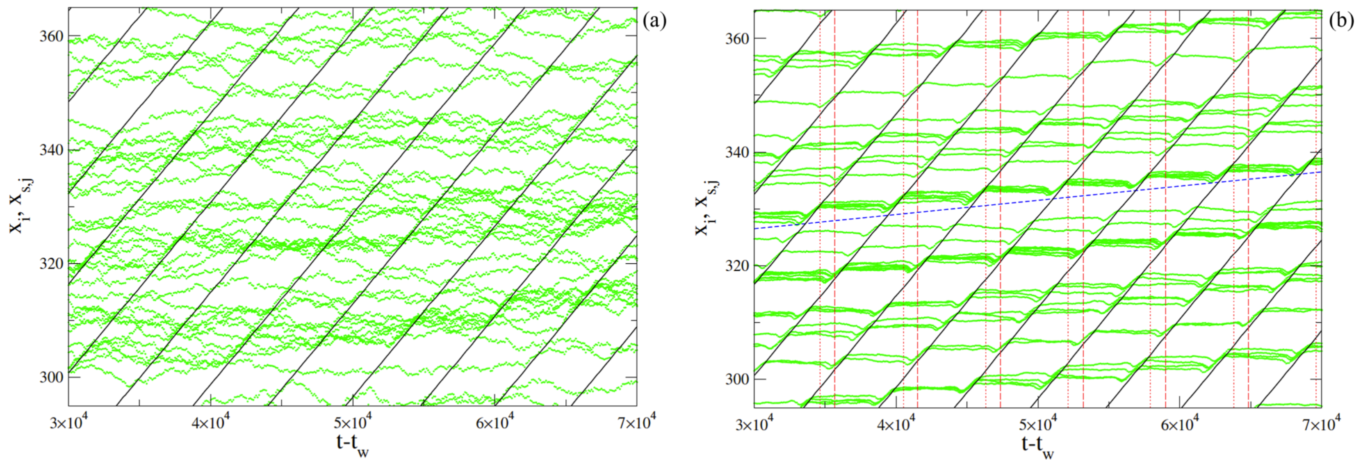

FIG. 5. (Color online) Representative portion of dislocations and pinning center motion for a single realization of the dynamics for the following parameter values: $V = 0.003$, $\mu/\chi = 0.5$, and (a) $1/T = 4 \times 10^2$ and (b) $1/T = 10^4$. The dark diagonal lines, with a slope equal to $V = 0.003$, are dislocations, and the green lines are pinning centers. (b) Dotted and dashed vertical (red) lines correspond to times for which the average stress has a minimum and a maximum, respectively. The horizontal dashed (blue) line, $y \sim v_{\mathrm{drift}}$, indicates the drift of pinning centers that move at velocity $v_{\mathrm{drift}} \simeq 2.5 \times 10^{-4}$.

number of pinning centers around dislocations, that is, $\langle N_p \rangle = N_p/N = 8$, which confirms directly that in these cases all pinning centers are pinning dislocations. Computing the standard deviation of the average distribution in Fig. 4 confirms that when serration emerges, for $1/T = 10^4$, dislocations depin in a coherent way. Indeed, in this case the standard deviation is big near the peak of the distribution but quite small away from it. In cases in which serration is not observed, for $1/T = 10^4$ and 4×10^2, the standard deviation is almost constant in time and space. Considering this result and that, in particular for $1/T = 4 \times 10^2$, the time ratio t_a/t_c (see Table I) is the same as for the case $1/T = 10^4$ and that the average curve is constant in time, we can conclude that when serration disappears, this means that dislocations depin in a incoherent way (at different times).

In Fig. 5 we see a representative portion of dislocation and pinning center motion in a case in which serration is not present [Fig. 5(a)] and case in which it appears [Fig. 5(b)]. The black lines are dislocations. They have a slope equal to $V = 0.003$, unless there are small deviations in the correspondence of pinning centers (the green lines) pinning dislocations. In Fig. 5(b) the vertical dotted and dashed (red) lines correspond to times for which the average stress has a minimum and a maximum, respectively. The minimum in the average stress corresponds to many dislocations that are pinned; the successive maximum, to many dislocations that depin. These processes are also present at intermediate times, which cause the appearance of small oscillations in the average stress between a big peak and a big valley [see Figs. 1 and 2(d)]. The dashed (blue) line, $y \sim v_{\mathrm{drift}} t$, indicates the drift of pinning centers that move at velocity $v_{\mathrm{drift}} \simeq 2.5 \times 10^{-4}$. This drift is caused by the interaction with dislocations.

In Fig. 6 we can see the entire dynamics of all dislocations in a case in which there is no serration [Fig. 6(a)] and another

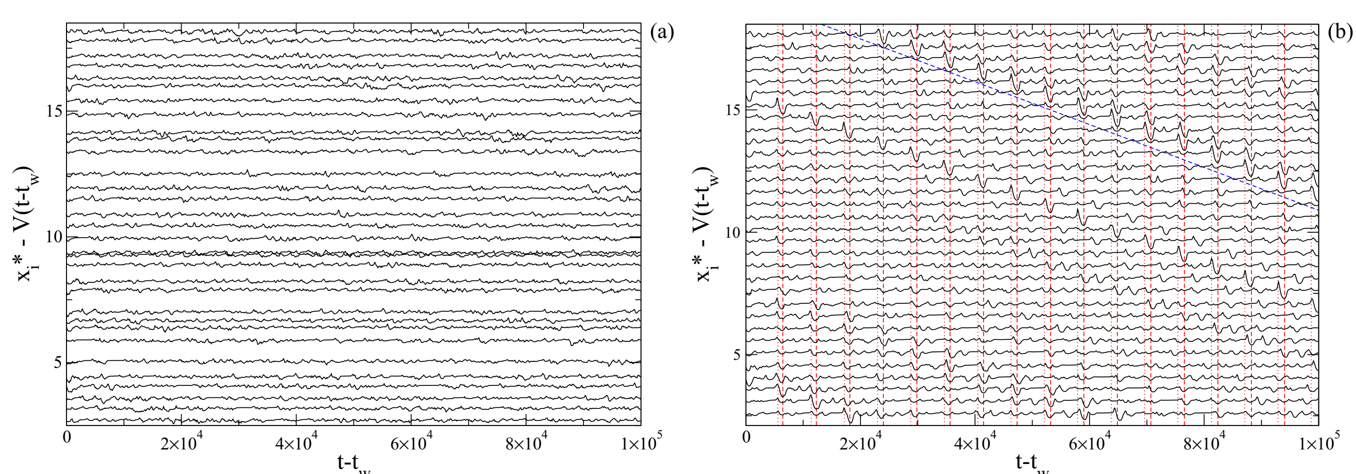

FIG. 6. (Color online) Dynamics of all dislocations for a single realization of the dynamics for the following parameter values: $V = 0.003$, $\mu/\chi = 0.5$, and (a) $1/T = 4 \times 10^2$ and (b) $1/T = 10^4$. To demonstrate fluctuations, the dislocation positions, at which the term Vt has been subtracted, are rescaled in such a way that the average interdistance between them is 0.5 instead of $d = 16$. (b) The diagonal dashed (blue) line, $y \sim -0.5/[d/(V - v_{\mathrm{drift}})]x = -0.875 \times 10^{-4}x]$, indicates clustering properties of pinning centers, as discussed in the text.

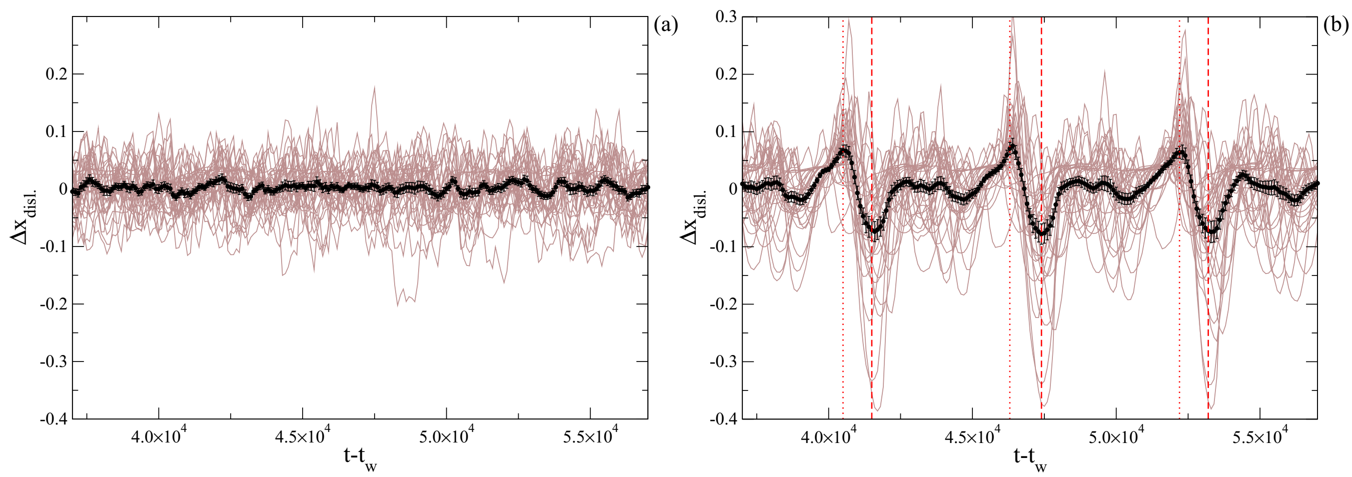

FIG. 7. (Color online) With the lighter color (brown) we display the superposition of the position fluctuations of all dislocations, $\Delta x_i = (x_i - Vt) - \langle (x_i - Vt) \rangle_t$, where the positions x_i are shown in Fig. 6, and the time average is performed on the entire dynamics. The black curve shows the average of all Δx_i, with the relative standard deviation. (b) Vertical dotted and dashed (red) lines correspond to times for which the average stress has a minimum and a maximum, respectively.

in which it appears [Fig. 6(b)]. In particular, the term Vt is subtracted from dislocation positions, so we have horizontal lines, while in Fig. 5 we have lines with a slope equal to V. Moreover, the positions of dislocations are rescaled in order to have an average interdistance between them of 0.5 instead of $d = 16$. The latter rescaling was done to demonstrate the fluctuations of dislocation position. As in Fig. 5, the vertical dotted and dashed (red) lines correspond to times for which the average stress has a minimum and a maximum, respectively. In Fig. 6(b) we see essentially two interesting things: minimum and maximum values in the rescaled dislocation position correspond to maximum and minimum values in the average stress, respectively; and the fluctuation profile of the position of one dislocation (in correspondence of serration) can propagate at a velocity of $V - v_{\text{drift}}$. The latter point means that when pinning centers start to cluster, they usually remain clustered during the entire dynamics. The dashed (blue line), $y \sim -0.5/[d/(V - v_{\text{drift}})]x = -0.875 \times 10^{-4}x$, in Fig. 6(b) indicates this behavior of pinning centers.

In Fig. 7 we display the superposition of fluctuations in the positions of all dislocations, Δx_i, in a case in which there is no serration [Fig. 7(a)] and another in which it appears [Fig. 7(b)]. These fluctuations were obtained as $\Delta x_i = (x_i - Vt) - \langle (x_i - Vt) \rangle_t$, where the time average is performed on the entire dynamics. We also display the average of all Δx_i, with the relative standard deviation, and the vertical dotted and dashed lines correspond to times for which the average stress has a minimum and a maximum, respectively. We can see another time that the minimum and maximum values of the average fluctuation position correspond to the maximum and minimum of the average stress, respectively.

VII. DISCUSSION

We have investigated the dynamics of a dislocation assembly interacting with mobile impurities by studying the case of a 1D dislocation pileup. In order to connect this model to the PLC effect, we studied the stress response of the system under an external constant strain rate. The free parameters of the system have been reduced to the driving velocity V, which controls the imposed constant strain rate, the mobility ratio μ/χ between dislocations and mobile impurities, and the temperature T. To this end, we have employed an effective definition of temperature that should be valid except at low temperatures and high stresses. Analyzing the average stress of the system $\langle \sigma \rangle$ in the parameter space $(V,\mu/\chi,1/T)$, we found a region characterized by stationary fluctuations in the stress (serration) (see Fig. 3).

The interpretation of the onset of serration in the present model agrees with the general concept of dynamic strain aging but takes explicitly into account the role of dislocation mutual interactions. The emergence of serration corresponds to the situation in which impurities diffuse at a rate that allows them to pin dislocations (i.e., the capturing time t_c is not too high). At the same time dislocations should be able to escape from pinning centers after an aging time t_a, which implies that t_a is not too high—otherwise, when dislocations unpinned, they would move at a high speed until they were arrested again and pinning centers would not be able to reach them—but also not too low, because in that case pinning centers would not be able to pin dislocations. Serration corresponds to the case in which the two characteristic time scales, t_a and t_c, are of the same order of magnitude (see Table I).

From another point of view, the origin of serration, over a specific range of parameter values $(V,\mu/\chi,T)$, is due to the localization of impurities in a limited number of clouds under the action of dislocation induced stresses and to the possibility of dislocations escaping from their pinning clouds without randomizing excessively the spatial distribution of impurities. The spatial localization of pinning centers is only possible due to the coherent action of several interacting dislocations. If we randomize the interaction between dislocations, for instance, by choosing Burgers vectors b_i for each dislocation i from a bounded random distribution, serration disappears. Spatial randomization of pinning centers results in an incoherent contribution to the total stress fluctuations of each dislocation, in the impossibility of clouds of pinning centers forming, and, therefore, in the disappearance of serration. Only when the contribution of each dislocation to the total stress fluctuations is coherent is serration observed.

The PLC effect displays many specific complex features that it is not possible to address using the present model. For example, in polycrystals, serration can be classified into three types of bands (A, B, C) [16]. They correspond to different dynamics of strain localization evolving from type C to type B and to type A when the strain rate is increased or the temperature is decreased. By calculating the correlation dimension and the Lyapunov spectrum of several sets of experimental time series data, it has been concluded that the PLC stress serrations are chaotic for low and medium strain rates and follow a power-law dynamics for high strain rates [25,43,44]. Furthermore, these studies show that there exists a correspondence between chaos and type B bands observed at low and medium strain rates, while the power-law regime present at high strain rates can be identified with type A bands. This complex dynamical behavior is likely to arise from the interaction of dislocations along different slip planes or from the possibility that pinning centers have a range of mobilities. Including similar ingredients in the model could give rise to different types of serrations observed under experimental conditions where A, B, and C bands can be identified. A possible way to identify other DDD mechanisms relevant to understanding all complex features of serration is to follow the method suggested by Groma in Ref. [45]: construct a dynamical equation for the coarse-grained dislocation density and compare it to the phenomenological equations developed for study of the PLC effect [25].

ACKNOWLEDGMENT

S.Z. was supported by the European Research Council through the Advanced Grant SIZEFFECTS.

[1] M. Zaiser, Adv. Phys. **55**, 185 (2006).
[2] J. Weiss and J. R. Grasso, J. Phys. Chem. B **101**, 6113 (1997).
[3] M.-C. Miguel, A. Vespignani, S. Zapperi, J. Weiss, and J. R. Grasso, Nature **410**, 667 (2001).
[4] M.-C. Miguel, A. Vespignani, M. Zaiser, and S. Zapperi, Phys. Rev. Lett. **89**, 165501 (2002).
[5] M. Z. Butt and P. Feltham, J. Mater. Sci. **28**, 2557 (1993).
[6] H. Neuhäuser, Phys. Scr. **T49B**, 412 (1993).
[7] F. Leoni and S. Zapperi, Phys. Rev. Lett. **102**, 115502 (2009).
[8] J. W. Cahn, Acta Metall. **10**, 789 (1962).
[9] D. Blavette, E. Cadel, A. Fraczkiewicz, and A. Menand, Science **286**, 2317 (1999).
[10] E. M. Chudnovsky, Europhys. Lett. **43**, 445 (1998).
[11] A. Portevin and F. Le Chatelier, C. R. Acad. Sci. Paris **176**, 507 (1923).
[12] A. Kalk and Ch. Schwink, Phys. Stat. Sol. (b) **172**, 133 (1992).
[13] A. Kalk and Ch. Schwink, Philos. Mag. A **72**, 315 (1995).
[14] F. Springer, A. Nortmann, and Ch. Schwink, Phys. Stat. Sol. (a) **170**, 63 (1998).
[15] K. Chihab, Y. Estrin, L. P. Kubin, and J. Vergnol, Scr. Metall. **21**, 203 (1987).
[16] P. Hähner, A. Ziegenbein, E. Rizzi, and H. Neuhäuser, Phys. Rev. B **65**, 134109 (2002).
[17] A. H. Cottrell and B. A. Bilby, Proc. Phys. Soc. A **62**, 49 (1949); A. H. Cottrell, Philos. Mag. **44**, 829 (1953).
[18] L. P. Kubin and Y. Estrin, Acta Metall. **33**, 397 (1985).
[19] P. Penning, Acta Metall. **20**, 1169 (1972).
[20] P. G. McCormick, Acta Metall. **21**, 873 (1973).
[21] A. van den Beukel, Phys. Stat. Sol. (a) **30**, 197 (1975).
[22] A. W. Sleeswyk, Acta Metall. **6**, 598 (1958).
[23] A. van den Beukel, Acta Metall. **28**, 965 (1980).
[24] N. Louat, Scr. Metall. **15**, 1167 (1981).
[25] G. Ananthakrishna, Phys. Rep. **440**, 113 (2007).
[26] H. Neuhäuser, in *Dislocations in Solids*, edited by F. R. N. Nabarro (North-Holland, Amsterdam, 1983).
[27] V. Mohles, Mater Sci. Eng. **309–310**, 265 (2001).
[28] G. Monnet, Philos. Mag. **86**, 5927 (2006).
[29] F. F. Csikor, C. Motz, D. Weygand, M. Zaiser, and S. Zapperi, Science **318**, 251 (2007).
[30] B. Devincre, T. Hoc, and L. Kubin, Science **320**, 1745 (2008).
[31] J. Senger, D. Weygand, P. Gumbsch, and O. Kraft, Scr. Mater. **58**, 587 (2008).
[32] B. Liu, D. Raabe, P. Eisenlohr, F. Roters, A. Arsenlis, and G. Hommes, Acta Mater. **59**, 7125 (2011).
[33] G. P. Reddy, C. Robertson, C. Depres, and M. Fivel, Acta Mater. **61**, 5300 (2013).
[34] C. Bairnsfather, C. J. Olson Reichhardt, and C. Reichhardt, Europhys. Lett. **94**, 18001 (2011).
[35] L. Laurson and M. J. Alava, J. Stat. Mech. (2008) P07003.
[36] H. Risken, *The Fokker-Plank Equation* (Springer Verlag, Berlin, 1984).
[37] M. F. Kanninen and A. R. Rosenfield, Philos. Mag. **20**, 569 (1969).
[38] J. P. Hirth and J. Lothe, *Theory of Dislocations* (Wiley & Sons, New York, 1982).
[39] B. Marcos and T. Baertschiger, M. Joyce, A. Gabrielli, and F. Sylos Labini, Phys. Rev. D **73**, 103507 (2006).
[40] F. J. Dyson, J. Math. Phys. **3**, 1191 (1962).
[41] M. Lebyodkin, L. Dunin-Barkovskii, Y. Bréchet, Y. Estrin, and L. P. Kubin, Acta Mater. **48**, 2529 (2000).
[42] S. Papanikolaou, D. M. Dimiduk, W. Choi, J. P. Sethna, M. D. Uchic, C. F. Woodward, and S. Zapperi, Nature **490**, 517 (2012).
[43] S. J. Noronha, G. Ananthakrishna, C. Fressengeas, and L. P. Kubin, Int. J. Bifurcat. Chaos **07**, 2577 (1997).
[44] S. Venkadesan, M. C. Valsakumar, K. P. N. Murthy, and S. Rajasekar, Phys. Rev. E **54**, 611 (1996).
[45] I. Groma, Phys. Rev. B **56**, 5807 (1997).